



HAL
open science

A rainfall simulator using porous pipes as drop former

Lionel Cottenot, Pierre Courtemanche, Amina Nouhou Bako, Frédéric Darboux

► **To cite this version:**

Lionel Cottenot, Pierre Courtemanche, Amina Nouhou Bako, Frédéric Darboux. A rainfall simulator using porous pipes as drop former. *CATENA*, 2021, 200, pp.105101. 10.1016/j.catena.2020.105101 . hal-03128470

HAL Id: hal-03128470

<https://hal.science/hal-03128470>

Submitted on 13 Feb 2023

HAL is a multi-disciplinary open access archive for the deposit and dissemination of scientific research documents, whether they are published or not. The documents may come from teaching and research institutions in France or abroad, or from public or private research centers.

L'archive ouverte pluridisciplinaire **HAL**, est destinée au dépôt et à la diffusion de documents scientifiques de niveau recherche, publiés ou non, émanant des établissements d'enseignement et de recherche français ou étrangers, des laboratoires publics ou privés.



Distributed under a Creative Commons Attribution - NonCommercial 4.0 International License

1

2

A rainfall simulator using porous pipes as drop former

3

4 Lionel Cottenot^{1,*}, Pierre Courtemanche¹, Amina Nouhou-Bako¹, Frédéric
5 Darboux^{1,2}

6

7 ¹ INRAE, URSOLS, 45075 Orléans, France.

8 ² Presently at: Univ. Grenoble Alpes, INRAE, ETNA, F-38402 St-Martin-d'Hères,
9 France.

10 *Corresponding author: Lionel Cottenot (lionel.cottenot@inrae.fr)

11 INRAE, UR Sols, CS 40001 – Ardon, 45075 Orléans, Cedex 2, France.

12

13 Highlights

- 14 • Design of a drop-former rainfall simulator using porous pipes
- 15 • Easier to build and maintain than rainfall simulators using capillaries
- 16 • Performances in the range of previous designs

17 Abstract

18 A drop-former rainfall simulator was designed and tested. Its novelty is the use of
19 porous pipes instead of capillaries. Compared to rainfall simulators using
20 capillaries, this feature makes easier its building and maintenance. Rainfall
21 intensity can be selected by simply setting the water supply pressure. The rainfall
22 simulator was able to deliver rainfall intensities between 24 and 75 mm/h for a
23 pressure range of 0.25-1.40 bar. As other drop-former rainfall simulators, the

24 rainfall kinetic energy (expressed in $\text{J}\cdot\text{m}^{-2}\cdot\text{mm}^{-1}$) and drop size do not depend on
25 the rainfall intensity. Tested on a 0.25 m^2 area, larger format could be build.

26

27 **Keywords:**

28 Rainfall simulator, drop former instrument, raindrop, kinetic energy

29

30 **1. Introduction**

31 Rainfall simulators are widely used in surface hydrology and in soil science
32 (Iserloh et al., 2013; Kesgin et al., 2018; Nielsen et al., 2019). While they come in
33 many variations, there are two basic types of rainfall simulators: nozzle-based and
34 drop-former (Iserloh et al., 2013).

35 The present paper describes a drop-former simulator. While drop-former
36 simulators typically make use of capillaries (needles, holes or small tubes), the
37 present design uses porous-pipes to generate the drops.

38 While our laboratory have used for years an oscillating-nozzle simulator (Foster et
39 al., 1979), an experiment required (1) a continuous rainfall over a surface of
40 0.25 m^2 , and (2) that rainfall intensity could be changed without altering the other
41 rainfall properties (kinetic energy, drop size). Aware of the complexity of
42 (1) building a regular drop-former rainfall simulator (with its hundreds to thousands
43 of capillaries per square meter) and (2) maintaining it (especially the clogging of
44 the capillaries) over long periods, we came with a new design that replace the
45 capillaries with porous pipes.

46 After detailing the design of the porous-pipe rainfall simulator, its performances are
47 evaluated and its use is discussed.

48 **2. Materials and methods**

49 **2.1 Design**

50 The design of the present porous-pipe rainfall simulator is part of the drop-former
51 rainfall simulator category. Basically, the capillaries and their specifically-designed
52 water supply are replaced by porous pipes connected to a manifold pipe.

53 Porous pipes are cheap and commonly used in gardens and horticulture for
54 irrigation. They are similar to water hoses, and can be bought in any garden shop.
55 They may come in different brands and specifications. The one used here is made
56 of a rubber-like material, with an outside diameter of 16 mm and an inside
57 diameter of 13 mm.

58 For our simulator, 25 sections of porous pipe of 0.9 meter long are used (Fig. 1).
59 They are lined up parallel to each other, with an inter-pipe spacing of 24 mm. One
60 end of the porous pipe section is blocked with a stopper, while the other end is
61 connected to a manifold pipe.

62 The porous pipes are placed under a one meter square sheet of expanded metal,
63 and attached to the sheet with plastic tie straps every 20 mm. The sheet of
64 expanded metal provides both a rigid frame and attachment holes for the tie straps.
65 The tie straps are key in achieving a homogeneous spatial distribution of the drops:
66 they collect the water coming out of the pipes and are the location where falling
67 drops are formed.

68 The manifold is connected to a water pump. A digital manometer is installed on the
69 manifold to allow for pressure monitoring and adjustment of the rainfall intensity.

70 Like in Ulrich et al. (2013) and Mayerhofer et al. (2017), a fine mesh (square 3 mm
71 openings, wire diameter of 0.5 mm) is placed 65 cm below the drop former device.

72 This mesh has two purposes: breaking the big drops into smaller drops, and

73 avoiding the drops to constantly fall onto the exact same location of the
74 experimental surface.

75 The porous pipes of the rainfall simulator are set 6.60 m above the experimental
76 area.

77 **2.2 Rainfall properties assessment**

78 36 pluviometers (cylindrical beakers of 64.5 mm in diameter and 110 mm in height)
79 are used to assess the intensity and spatial variability of the rain inside a central
80 area of 50 cm by 50 cm, which is the size of the test bench to be used in
81 subsequent experiments. The collected amount of water is measured by weighting
82 the pluviometers. The uniformity coefficient of Christiansen is calculated (Iserloh et
83 al., 2013).

84 For the drop size and the rainfall kinetic energy, an optical disdrometer is used
85 (Laser Precipitation Monitor, Thies clima, part number 5.4110.00.XXX). This
86 disdrometer senses the drops crossing a laser beam and reports their number,
87 sizes and falling speeds every minute. It is located in the center of the test area.
88 During preliminary tests, an underestimation of the rainfall intensity by the
89 disdrometer was found, as previously reported (Prata de Moraes Frasson *et al.*,
90 2011; Angulo-Martinez *et al.*, 2018). Hence, kinetic energies are linearly
91 compensated based on the differences between disdrometer intensity and
92 pluviometer intensity.

93 Rainfall properties are assessed at four water pressures (0.25, 0.50, 0.86, and
94 1.40 bar). Three replicates were carried out for the 0.86-bar pressure to assess the
95 reproductibility of the rainfall intensity.

96 **3. Results and discussion**

97 For the range of pressure 0.25–1.40 bar, rainfall intensity varied between 24 and
98 75 mm/h (Table 1). The dependency of the intensity to the water pressure was
99 mostly linear, making it easy to reach a prescribed intensity. The variability of the
100 rainfall intensity was about 10% between replicates, which is in the usual range for
101 rainfall simulators (Iserloh et al., 2013). The uniformity coefficient of Christiansen is
102 always above 90%, which is in the higher range compared with other rainfall
103 simulators (Iserloh et al., 2013). The spatial variability of rainfall intensity showed a
104 gradient along the direction of the porous pipes (Fig. 2): compared to the mean
105 value, the intensity was lower by 7% on the half of the test surface located to the
106 manifold side, and higher by 7% on the half of the test surface located on the
107 stopper side. This gradient was mostly independent of the rainfall intensity.

108 The simulator produced droplets with a mean weighted diameter of 3.0 mm. This
109 value did not change with the rainfall intensity. This is typical of drop-former rainfall
110 simulators which, by design, cannot alter their drop size (except by changing the
111 wire mesh).

112 The drop velocities were independent of the rainfall intensity (data not shown).
113 Drop-former rainfall simulators generates drops with an initial zero velocity. During
114 their fall, drops interact with the wire mesh and accelerate due to gravity. Hence
115 their final velocity depends simply of their size and falling height.

116 Rainfall kinetic energies were in the range of 18-23 J.m⁻².mm⁻¹ (Table 1). These
117 values are quite close, meaning that the kinetic energy of the rain did not depend
118 on the rainfall intensity. This was expected because (1) drop sizes and velocities
119 were constant whatever the water pressure, and (2) the kinetic energy is
120 expressed by millimeter of rainfall. The obtained kinetic energies are higher than in

121 the previously-reported range (Iserloh et al., 2013), owing to the larger drop fall
122 height.

123 Overall, the results are in accordance with the expected behavior of a drop-former
124 rainfall simulator, validating the present design for further use. The present design
125 allows changing the rainfall characteristics independently: rainfall intensity
126 depends on the water supply pressure, while the drop size and kinetic energy
127 depends on mesh size and falling height. This feature could be advantageous to
128 study the sensitivity of processes (such as particle splash or herbicide transfer) to
129 the different rainfall properties.

130 Upon designing and using this simulator, we encountered several issues that
131 should draw attention:

- 132 • The porosity of the hose roll may not be constant along its length. It may
133 depends on the batch and on the brand. Hence, after testing, some 0.9 m
134 sections have been discarded.
- 135 • On start-up, the rainfall intensity may be lower than expected: the porous
136 pipes need to be moistened before they provide a constant water flow.
137 Hence, the simulator needs to be run for a few minutes before being fully
138 functional. By contrast, the rainfall stops instantaneously when the water
139 supply pipe is disconnected from the pump.
- 140 • As underlined earlier, the intensity is lower on the manifold side than on the
141 stopper side. If this rainfall intensity gradient is too high compared to the
142 requirements, two manifolds could be used, supplying water from both
143 sides of the porous pipes.
- 144 • For a given pressure, rainfall intensity decreases over the course of several
145 weeks. This could be due to aging and clogging of the porous pipes
146 (Teeluck and Sutton, 1998). With a few exceptions, such as Battany and

147 Grismer (2000), clogging is rarely mentioned in publications about drop-
148 former rainfall simulators. However, this issue is well-known to users.
149 Clogging results in a decrease of the rainfall intensity and an increase of its
150 spatial variability. For the present design, such inconvenience could be slow
151 down by adding a water filter (Teeluk et al., 1998). Such an effect should be
152 monitored, and, if significant, porous pipes can be easily replaced with new
153 ones. While clogging occurs with porous pipes as with needles, it is much
154 easier and faster to change the 25 porous pipes of the present design than
155 the hundreds of capillaries of previous designs.

156 Overall, the porous-pipe rainfall simulator allows to generate a continuous rain,
157 with drops of significant size, velocity and kinetic energy, having a random
158 distribution of the impact points, for a significant range of rainfall intensities, and a
159 limited spatial heterogeneity over a square surface of 0.25 m².

160 Potentially, the current design may be extended to provide rainfall over larger
161 surfaces. This may be achieved by using longer or more numerous sections of
162 porous pipes. As a reference, drop-former rainfall simulators exist for areas of
163 0.06 m², using 49 capillaries (Kamphorst, 1987) to areas of 6 m², using
164 4800 capillaries (Huang et al., 2016). We believe large drop-former rainfall
165 simulators could advantageously use porous pipes instead of capillaries.

166 **4. Conclusions**

167 A rainfall simulator based on porous pipes was designed and tested. It can
168 generate rainfall intensities between 24 and 75 mm/h. Rainfall intensity can easily
169 be preset by choosing the water supply pressure. Rainfall kinetic energy
170 (expressed in J.m⁻².mm⁻¹) and drop size do not depend on the rainfall intensity.
171 The given advises will make easier its building and use. Compared to rainfall

172 simulators using capillaries, design and maintenance are easier. Tested on a 0.25-
173 m² area, it could be expanded to larger surfaces.

174

175 **Competing interests:** authors declare no competing interests.

176

177 **Funding:** This work was supported by French National Research Institute for
178 Agricultural, Food and Environment and the Conseil Régional du Centre-Val de
179 Loire.

180

181 **References**

182 Angulo-Martinez, M., Begueria, S., Latorre, B., Fernández-Raga, M. (2018).

183 Comparison of precipitation measurements by OTT Parsivel² and Thies LPM
184 optical disdrometers. *Hydrology and Earth System Sciences*. 22, 2811–2837.
185 <https://doi.org/10.5194/hess-22-2811-2018>.

186 Battany, M. C., Grismer, M. E. (2000). Development of a portable field rainfall
187 simulator for use in hillside vineyard runoff and erosion studies. *Hydrological
188 Processes*. 14, 1119–1129. [https://doi.org/10.1002/\(SICI\)1099-
189 1085\(20000430\)14:6%3C1119::AID-HYP8%3E3.0.CO;2-O](https://doi.org/10.1002/(SICI)1099-1085(20000430)14:6%3C1119::AID-HYP8%3E3.0.CO;2-O).

190 Foster, G. R., Eppert, F. P., Meyer, L. D. (1979). A programmable rainfall simulator
191 for field plots. *Proceedings of the Rainfall Simulator Workshop*. Tucson, Arizona.
192 March 7–9, Agricultural Reviews and Manuals, ARM-W-10. United States
193 Department of Agriculture – Science and Education Administration, Oakland,
194 CA, 45–59.

195 Huang, J., Wang, J., Zhao, X., Li, H., Jing, Z., Gao, X., Chen, X., Wu, P. (2016).
196 Simulation study of the impact of permanent groundcover on soil and water

197 changes in jujube orchards on sloping ground. *Land Degradation &*
198 *Development*, 27, 946-954. <https://doi.org/10.1002/ldr.2281>.

199 Iserloh, T.; Ries, J. B.; Arnáez, J.; Boix-Fayos, C.; Butzen, V.; Cerdà, A.;
200 Echeverría, M. T.; Fernández-Gálvez, J.; Fister, W.; Geißler, C.; Gómez, J. A.;
201 Gómez-Macpherson, H.; Kuhn, N. J.; Lázaro, R.; León, F. J.; Martínez-Mena, M.;
202 Martínez-Murillo, J. F.; Marzen, M.; Mingorance, M. D.; Ortigosa, L.; Peters, P.;
203 Regüés, D.; Ruiz-Sinoga, J. D.; Scholten, T.; Seeger, M.; Solé-Benet, A.;
204 Wengel, R. & Wirtz, S. (2013). European small portable rainfall simulators: A
205 comparison of rainfall characteristics. *Catena*, 110, 100–112.
206 <https://doi.org/10.1016/j.catena.2013.05.013>.

207 Kesgin, E., Dogan, A., Agaccioglu, H. (2018). Rainfall simulator for investigating
208 sports field drainage processes. *Measurement*, 125, 360–370.
209 <https://doi.org/10.1016/j.measurement.2018.05.001>.

210 Kamphorst, A. (1987). A small rainfall simulator for the determination of soil
211 erodibility. *Netherlands Journal of Agricultural Sciences*, 35, 407–415.

212 Nielsen, K. T., Moldrup, P., Thorndahl, S., Nielsen, J. E., Duus, L. B., Rasmussen,
213 S. H., Uggerby, M., Rasmussen, M. R. (2019). Automated rainfall simulator for
214 variable rainfall on urban green areas. *Hydrological Processes*, 33, 3364–3377.
215 <https://doi.org/10.1002/hyp.13563>.

216 Mayerhofer, C., Meißl, G., Klebinder, K., Kohl, B., Markart, G. (2017). Comparison
217 of the results of a small-plot and a large-plot rainfall simulator – Effects of land
218 use and land cover on surface runoff in Alpine catchments. *Catena*, 156, 184–
219 196. <https://doi.org/10.1016/j.catena.2017.04.009>.

220 Prata de Moraes Frasson, R., Kindl da Cunha, L., Krajewski, W. F. (2011).
221 Assessment of the Thies optical disdrometer performance. *Atmospheric*
222 *Research*, 101, 237–255. <https://doi.org/10.1016/j.atmosres.2011.02.014>.

- 223 Teeluck, M., Sutton, B. G. (1998). Discharge characteristics of a porous pipe
224 microirrigation lateral. *Agricultural Water Management*, 38, 123–134.
225 [https://doi.org/10.1016/s0378-3774\(98\)00060-2](https://doi.org/10.1016/s0378-3774(98)00060-2).
- 226 Ulrich, U., Zeiger, M., Fohrer, N. (2013). Soil structure and herbicide transport on
227 soil surfaces during intermittent artificial rainfall, *Zeitschrift für Geomorphologie*,
228 57, 135–155. <https://doi.org/10.1127/0372-8854/2012/s-00097>.

229 **List of tables**

230 Table 1: Rainfall properties at different water pressures.

231

232 **List of figures**

233 Fig. 1. Scheme of the rainfall simulator.

234 For clarity, the sheet of expanded metal is not drawn. Not to scale.

235

236 Fig. 2. Spatial variability of rainfall intensity at different water pressures.

237

Pressure (bar)	Intensity (mm/h)	Kinetic energy (J.m ⁻² .mm ⁻¹)	Coefficient of uniformity (%)
0.25	23.9 ± 2.5	18	92
0.50	36.0 ± 3.5	Not measured	93
0.86	49.0 ± 5.2	23	92
1.40	74.5 ± 6.9	23	92

240 Table 1: Rainfall properties at different water pressures.

242

243

244

245

246

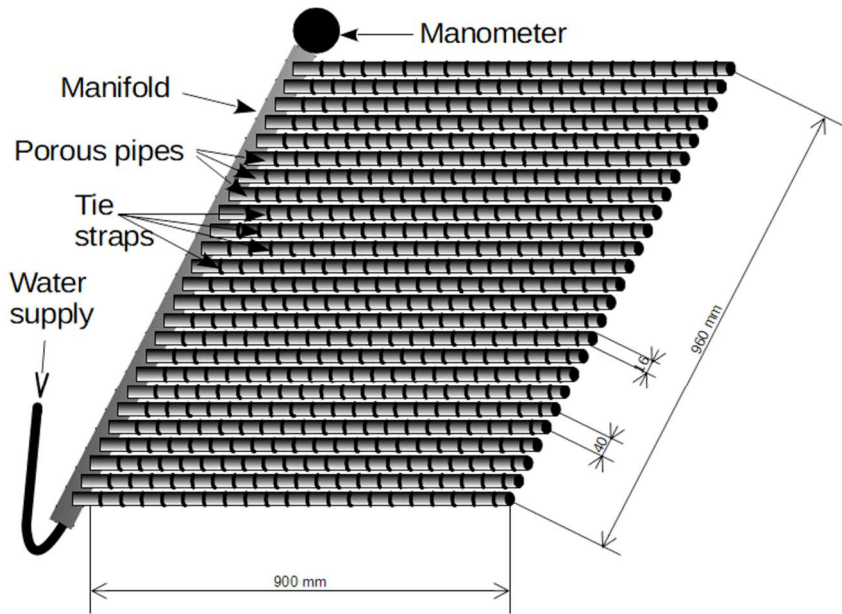
247

248

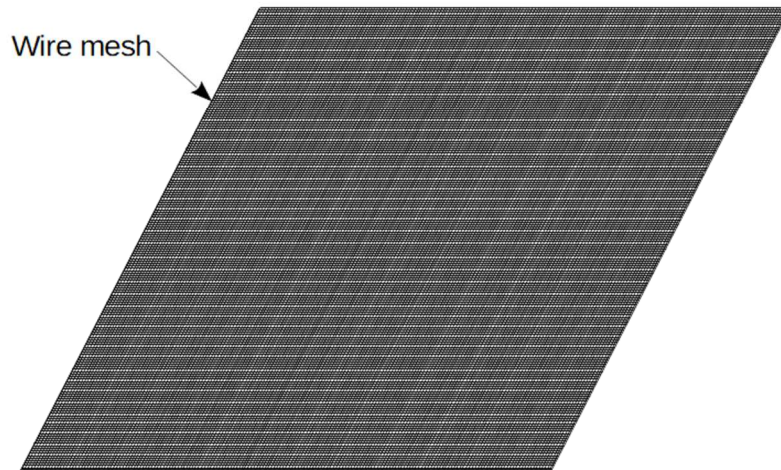
249

250

251



252



253

254

255

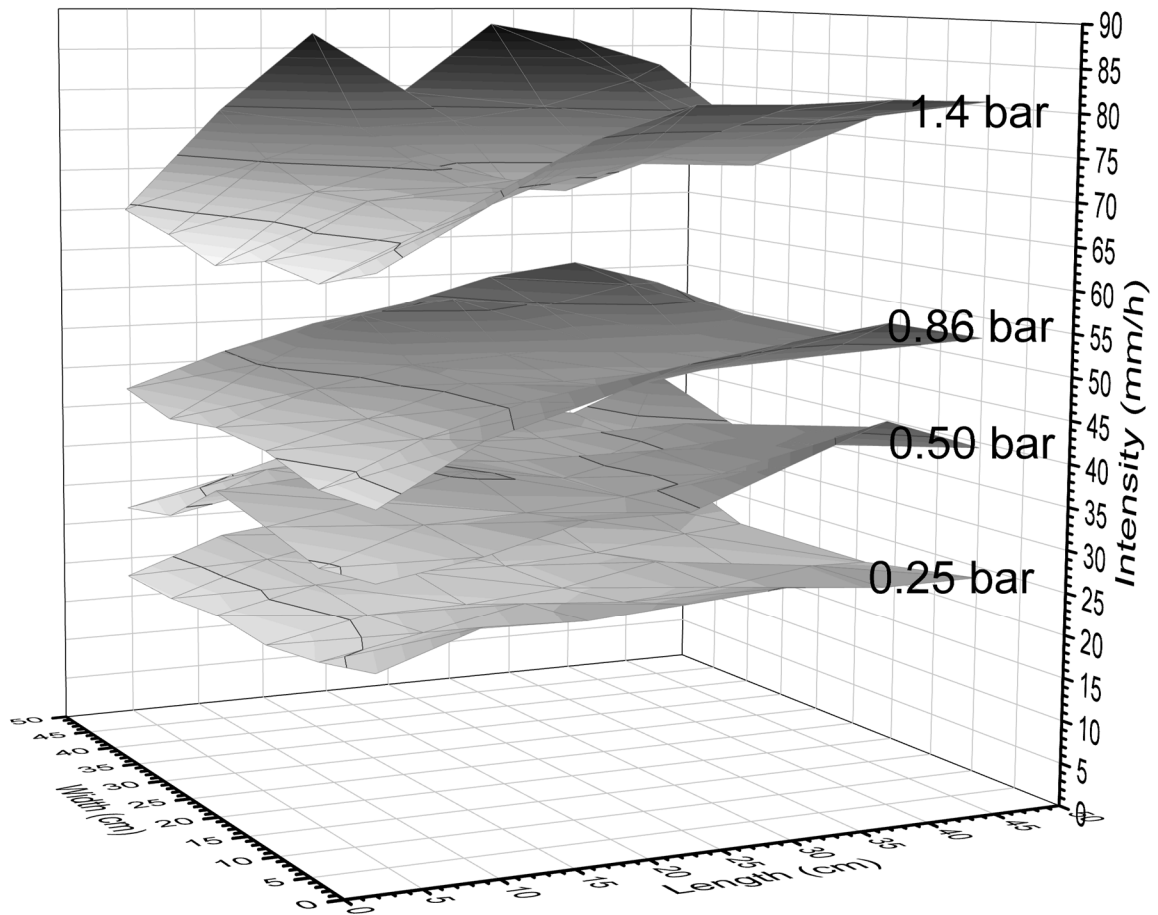
256

257

258

259 Fig. 1. Scheme of the rainfall simulator.

260 For clarity, the sheet of expanded metal is not drawn. Not to scale.



261 Fig. 2. Spatial variability of rainfall intensity at different water pressures.

262 The manifold is located to the left.